J. Am. Chem. Soc. 1985, 107, 91-97

which seems to account for all the experimental observations, is summarized in Figure 12. It should, however, be realized that the scheme presented in Figure 12 is still largely phenomenological. Structure–photoreactivity correlations of the excited states are yet to be unraveled, and the role of the quartet manifold, if any, in the photochemical pathways of the higher excited states is completely unknown.

Finally, the ability to monitor the absorption spectrum of D_1 could allow some significant observations on the energy levels of the radicals. In principle, due to parity selection rules, transitions which are forbidden for the ground state have to become symmetry-allowed in the first excited state. In the radicals for which the absorption spectra of D_1 were monitored, the lowest observable transition corresponds to excitation to a level which lies 5.3 eV above the ground state. Since neither experimental nor calculated information is available on the absorption spectrum of the ground state in this region, comparison at this stage between the absorption spectra of the two states is premature.

Acknowledgment. The dedicated operation of the linac by D. Ficht and G. Cox is gratefully acknowledged, as is the technical assistance of P. Walsh and R. Clarke.

Registry No. DBHP-OH, 1210-34-0; DBHP-Cl, 1210-33-9; DBHP·, 93564-50-2; Ph$_2$CHCl, 90-99-3; Ph$_2$CHOH, 91-01-0; Ph$_2$C(CH$_3$)OH, 599-67-7; Ph$_3$CCl, 76-83-5; Ph$_3$COH, 76-84-6; (c-Pr)ĊPh$_2$, 17787-94-9; Ph$_3$CH, 4471-17-4; Ph$_3$C·, 2216-49-1; Ph$_2$ĊCH$_3$, 51314-23-9; CH$_3$C≡N, 75-05-8; Ph$_2$C(c-Pr)OH, 5785-66-0; 1-(10,11-dihydro-5H-dibenzo[a,-d]cyclohepten-5-ylidene)ethyl amidogen, 93474-28-3.

(26) Sitzmann, E. V.; Wang, Y.; Eisenthal, K. B. *J. Phys. Chem.* **1983**, *87*, 2283.

Problems of CD Spectrometers. 3. Critical Comments on Liquid Crystal Induced Circular Dichroism

Yohji Shindo* and Yasuhiro Ohmi

Contribution from the Research Institute for Material Science and Engineering, Faculty of Engineering, Fukui University, Fukui 910, Japan. Received June 15, 1984

Abstract: The Mueller matrix approach is used to analyze the apparent circular dichroism (CD) spectra observed in cholesteric liquid crystals (CLC) which can be regarded as being built up of a large number of thin birefringent layers arranged helically. Attention is called to the artifacts resulting from coupling of CLC with nonideal optics and electronics of the CD spectropolarimeter. On the basis of the results obtained, it is concluded that "liquid crystal induced CD" cannot be related to true optical activity without careful consideration of the experiment.

More than 100 papers have been published since the first report on liquid crystal induced circular dichroism (LCICD) in 1971[1] and the number of papers is still increasing. Norden[2,3] and Jensen[4] called attention to the instrumental limitation of CD spectrometers in studying CD phenomena of liquid crystals and other systems with macroscopic anisotropy. They also demonstrated the usefulness of the Mueller matrix algebra for analyzing the data obtained. But their very important papers are frequently ignored, and LCICD spectra measured with commercial CD spectropolarimeters have been widely accepted as representing an induced optical activity of achiral molecules dissolved in cholesteric liquid crystals without any doubt. Is this really true? Our answer is "no", and the very reason for this is presented in this paper.

A paper by Tunis-Schneider et al.[5] has been used for the theoretical support of LCICD. But this work has the serious limitation of assuming that the CD spectrometer is ideal. In practice, however, there is no ideal CD spectrometer, whether it is commercially built or homemade. In our first paper of this series,[6] we show that a modern CD spectrometer is fundamentally a polarization–modulation spectrometer with the systematic errors inevitable in polarization–modulation techniques due to a partially polarizing detector, residual static strain birefringence of the
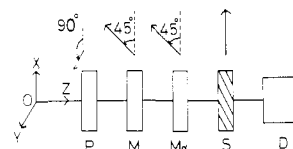

Figure 1. Optical arrangements showing the orientation of the optical components: P, polarizer; M, PEM; M_α, residual static strain retardation of PEM; S, sample; D, photomultiplier.

electrooptical modulator, and a first harmonic response of a lock-in amplifier. Even in an ideal CD spectrometer, their discussion is valid only under the very restricted condition that linear dichroism (LD) and linear birefringence (LB) of the sample are small. But the linear effects of liquid crystals are, in reality, by no means small. In the previous paper,[7] we considered the artifacts resulting from the coupling of an anisotropic medium and nonideal optics and electronics of the CD spectrometer. Therefore, the method of analyzing apparent CD data proposed by Tunis-Schneider et al. can in practice never be applied to liquid crystals and other systems with macroscopic anisotropy.

In this paper, we focus our attention to the apparent CD signals observed in cholesteric liquid crystals which can be regarded as build up of a large number of helically arranged thin birefringent layers. We investigate this problem by using the same Mueller matrix approach as described in our earlier papers. Our conclusion is that a LCICD spectra measured with commercially available CD spectrometers cannot generally be used as proof of optical

(1) Saeva, F. D.; Wysocki, J. J. *J. Am. Chem. Soc.* **1971**, *93*, 5928–5929.
(2) Norden, B. *J. Phys. Chem.* **1977**, *81*, 151–159.
(3) Davidsson, A.; Norden, B.; Seth, S. *Chem. Phys. Lett.* **1980**, 313–316.
(4) Jensen, H. P.; Schellman, J. A.; Troxell, T. *Appl. Spectrosc.* **1978**, *32*, 192–200.
(5) Tunis-Schneider, M. J. B.; Maester, M. F. *J. Mol. Biol.* **1970**, *52*, 521–541.
(6) Shindo, Y.; Nakagawa, M., *Rev. Sci. Insrum.*, in press.

(7) Shindo, Y.; Nakagawa, M. *J. Appl. Spectrosc.*, in press.

0002-7863/85/1507-0091$01.50/0   © 1985 American Chemical Society

activity induced in optically inactive molecules dissolved in cholesteric liquid crystals.

Theoretical Consideration and Discussion

Figure 1 shows the optical arrangement and axis orientation of the optical component used in our JASCO J-500 CD spectrometer. We can understand from the following example how versatile and powerful the Mueller matrix approach is for instrument design, analysis, and evaluation. The description of polarized light in common use is the Stokes vector which has four components;

$$\hat{S} = \begin{pmatrix} S_0 \\ S_1 \\ S_2 \\ S_3 \end{pmatrix} \tag{1}$$

For light which is monochromatic and contains no depolarizaed component, the components S_i are defined as

$$S_0 = P_x^2 + P_y^2 = I_x + I_y$$
$$S_1 = 2P_xP_y \cos \gamma$$
$$S_2 = 2P_xP_y \sin \gamma$$
$$S_3 = P_x^2 - P_y^2 = I_x - I_y \tag{2}$$

where P and γ stand for the amplitudes and phases of the field vectors. S_0 is called the intensity. The components S_1, S_2, and S_3 may be regarded as the "plus 45° preference", a "right circular preference", and "horizontal preference", respectively.[8] Therefore, the Stokes vector of the incident beam is given as

$$\hat{I}_{in} = \begin{pmatrix} 1 \\ 0 \\ 0 \\ 0 \end{pmatrix} \tag{3}$$

The Mueller matrix of the polarizer is

$$\hat{P} = \frac{1}{2}\begin{pmatrix} 1 & 0 & 0 & -1 \\ 0 & 0 & 0 & 0 \\ 0 & 0 & 0 & 0 \\ -1 & 0 & 0 & 1 \end{pmatrix} \tag{4}$$

The properties of the emerging beam are obtained by multiplying the vector describing the incident beam by the matrix describing the polarizer. Consequently,

$$\frac{1}{2}\begin{pmatrix} 1 & 0 & 0 & -1 \\ 0 & 0 & 0 & 0 \\ 0 & 0 & 0 & 0 \\ -1 & 0 & 0 & 1 \end{pmatrix}\begin{pmatrix} 1 \\ 0 \\ 0 \\ 0 \end{pmatrix} = \frac{1}{2}\begin{pmatrix} 1 \\ 0 \\ 0 \\ -1 \end{pmatrix} \tag{5}$$

The first element is $1/2$, indicating that the emerging beam has an intensity of $1/2$. The second and third terms are zero. The last term is negative, indicating a preference for horizontal polarization. Thus, we conclude that the resulting beam is 100% linearly and horizontally polarized. The Mueller matrix formalism of the photoelastic modulator (PEM) is given as

$$\hat{M}_{\delta + \alpha} = \begin{pmatrix} 1 & 0 & 0 & 0 \\ 0 & 1 & 0 & 0 \\ 0 & 0 & \cos(\delta + \alpha) & -\sin(\delta + \alpha) \\ 0 & 0 & \sin(\delta + \alpha) & \cos(\delta + \alpha) \end{pmatrix} \tag{6}$$

Here, δ is the periodic-phase difference between M_x and M_y axes of the modulator operating at frequency W_m (50 kHz for PEM used in the JASCO J-500 CD spectrometer,

$$\delta = \delta_m^° \sin W_m t \tag{7}$$

$\delta_m^°$ is the peak modulator retardation, which is adjusted so as to act as a quarter-wave plate. α is the residual static-phase dif-

ference in the optical element of the modulator head induced between x- and y-polarized waves. Similarly, we know the properties of the emerging light from the simple matrix calculation

$$\begin{pmatrix} 1 & 0 & 0 & 0 \\ 0 & 1 & 0 & 0 \\ 0 & 0 & \cos(\delta + \alpha) & -\sin(\delta + \alpha) \\ 0 & 0 & \sin(\delta + \alpha) & \cos(\delta + \alpha) \end{pmatrix}\begin{pmatrix} 1 \\ 0 \\ 0 \\ -1 \end{pmatrix} = \frac{1}{2}\begin{pmatrix} 1 \\ 0 \\ \sin(\delta + \alpha) \\ -\cos(\delta + \alpha) \end{pmatrix} \tag{8}$$

The emerging beam has an intensity of $1/2$. The third and fourth elements are $\sin(\delta + \alpha)$ and $-\cos(\delta + \alpha)$, respectively. What do these mean? They indicate preferences for circular and horizontal polarization which are modulated periodically. Using trigonometric expansion, we get

$$\sin(\delta + \alpha) = \sin \delta \cos \alpha + \cos \delta \sin \alpha$$
$$-\cos(\delta + \alpha) = -\cos \delta \cos \alpha + \sin \delta \sin \alpha \tag{9}$$

We can expand $\sin \delta$ and $\cos \delta$ in a Fourier series,

$$\cos \delta = \cos(\delta_m^° \sin W_m t) =$$
$$J_0\delta_m^° + 2J_2\delta_m^° \cos 2W_m t + ... \sin \delta = \sin(\delta_m^° \sin W_m t) =$$
$$2J_1\gamma\delta_m^° \sin W_m t + 2J_3\delta_m^° \sin 3W_m t + ... \tag{10}$$

where $J_k\delta_m^°$ are Bessel functions of the order k. Therefore,

$$\sin(\delta + \alpha) =$$
$$2J_1\delta_m^° \sin W_m t \cos \alpha + 2J_2\delta_m^° \cos 2W_m t \sin \alpha + J_0\delta_m^° \sin \alpha$$

$$-\cos(\delta + \alpha) =$$
$$2J_2\delta_m^° \cos 2W_m t \cos \alpha + 2J_1\delta_m^° \sin W_m t \sin \alpha - J_0\delta_m^° \cos \alpha \tag{11}$$

Since $\delta_m^°$ is adjusted to 1.83 rad, $J_0\delta_m^°$, $J_1\delta_m^°$, and $J_3\delta_m^°$ are equal to 0.32, 0.58, and 0.32, respectively. From these relationships, we know that unless α is equal to zero, that is, the modulator is ideal, there is always left and right circularly polarized components modulated at the frequencies W_m and $2W_m$ and a right circularly polarized, unmodulated component in the emerging light. Similarly, there exist vertically and horizontally polarized components modulated W_m and $2W_m$ and a horizontally polarized, unmodulated component in the light. Table I summarizes the α of the PEM and Pockel's cell used in our JASCO J-500 and a JASCO J-40 CD spectropolarimeter reported by Norden.[9,10] There is a wavelength dependence in α, and its values increases at shorter wavelengths. The α of Pockel's cell is 2 orders larger than that of our PEM, indicating its inferior performance as an optical modulator.

Once the Mueller matrix of a sample is formulized, we can easily get the information on the properties of the emergent light from the sample. Furthermore, it is not difficult to integrate the optical quantities of the sample such as the phase shift and absorbances into a Mueller matrix. These are the attractive features of the Mueller matrix approach. For air blank, the Mueller matrix is given as

$$\hat{S}(0) = \begin{pmatrix} 1 & 0 & 0 & 0 \\ 0 & 1 & 0 & 0 \\ 0 & 0 & 1 & 0 \\ 0 & 0 & 0 & 1 \end{pmatrix} \tag{12}$$

The properties of the light after passing through the sample are obtained as

$$\begin{pmatrix} 1 & 0 & 0 & 0 \\ 0 & 1 & 0 & 0 \\ 0 & 0 & 1 & 0 \\ 0 & 0 & 0 & 1 \end{pmatrix}\frac{1}{2}\begin{pmatrix} 1 \\ 0 \\ \sin(\delta + \alpha) \\ -\cos(\delta + \alpha) \end{pmatrix} = \frac{1}{2}\begin{pmatrix} 1 \\ 0 \\ \sin(\delta + \alpha) \\ -\cos(\delta + \alpha) \end{pmatrix} \tag{13}$$

There is, of course, no change observed in the emerging beam.

---

(8) Shurcliff, W. A. "Polarized Light"; Harvard University Press, Cambridge, MA 1962; pp 19–29.

(9) Davidsson, A.; Norden, B. *Spectrochim. Acta, Part A* **1976**, *32A*, 717–722.
(10) Davidsson, A.; Norden, B. *Chem. Scr.* **1976**, *9*, 49–53.

$$\hat{D} = \begin{pmatrix} P_x^2 + P_y^2 & (P_x^2 - P_y^2)\sin 2a & 0 & (P_x^2 - P_y^2)\cos 2a \\ (P_x^2 - P_y^2)\sin 2a & (P_x^2 + P_y^2)\sin^2 2a + 2P_xP_y\cos^2 2a & 0 & (P_x - P_y)^2\cos 2a \sin 2a \\ 0 & 0 & 2P_xP_y & 0 \\ (P_x^2 - P_y^2)\cos 2a & (P_y - P_y)^2\cos 2a \sin 2a & 0 & (P_x^2 + P_y^2)\cos^2 2a + 2P_xP_y\sin^2 2a \end{pmatrix} \quad (14)$$

Table I. Residual Static Strain Retardation of Our PEM and Pockel's Cell

	PEM			Pockel's cell		
λ_m	$\alpha°$	$\sin \alpha°$	$\cos \alpha°$	$\alpha°$	$\sin \alpha°$	$\cos \alpha°$
575	0.0127	2.2×10^{-4}	1	5.3	0.92×10^{-1}	0.996
550	0.0143	2.5	1	5.4	0.99	0.996
525	0.0138	2.4	1	5.7	1.01	0.995
500	0.0164	2.9	1	6.0	1.05	0.995
475	0.0218	3.8	1	6.3	1.10	0.994
450	0.0254	4.4	1	6.7	1.17	0.993
425	0.0283	4.9	1	7.0	1.22	0.993
400	0.0320	5.6	1	7.5	1.31	0.991
375	0.0394	6.9	1	8.0	1.38	0.990
350	0.0375	6.5	1	8.3	1.44	0.970

Table II. Polarization Characteristics of Our Photomultiplier

λ_m	$P_x^2 - P_y^2$	θ, millideg
560	2.5×10^{-4}	8.3
450	2.7×10^{-4}	9.0
350	8.1×10^{-3}	270
220	4.9×10^{-2}	1633

Table III. Apparatus Constant Related to the Gain of Lock-In Amplifier at 50 kHz

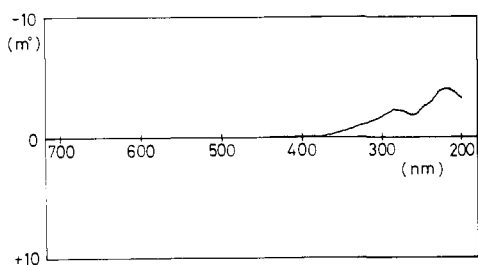| sensitivity, mdeg/cm	k	sensitivity, mdeg/cm	k
50	6.4×10^3	1	3.2×10^5
20	1.6×10^4	0.5	6.4×10^5
10	3.2×10^4	0.2	1.6×10^6
5	6.4×10^4	0.1	3.2×10^6
2	1.6×10^5		

Figure 2. Base-line shift of our JASCO J-500 CD spectropolarimeter with the base-line correction "off": sensitivity, 2 mdeg/cm.

If a photomultiplier was ideal, it would have no polarization characteristics; in other words, it would not act as a partial polarizer. In practice, however, there are no ideal photomultipliers. Thus, the Mueller matrix of the photomultiplier can be formulized as shown in eq 14 where P_x^2 and P_y^2 are the principal transmittances of the photomultiplier in the x and y directions and a is the azimuth angle of its optical axis with respect to the x axis.

From the above equation, we know that P_x^2 and P_y^2 are equal to $^1/_2$ for the ideal photomultiplier, and $P_x^2 \sim P_y^2$ and a show the polarization characteristics of the detector. O'Handley[11] reported $P_x^2 - P_y^2 = 0.0044$ for an EMI 9558 head-on-type photomultiplier. Since 1 millideg in the CD scale is equivalent to 3×10^{-5} optical density (OD), this value is about 150 millideg, which is fairly large on the CD scale.

Table II summarizes the values of $P_x^2 - P_y^2$ for the photomultiplier in our CD spectrometer.[6] $P_x^2 - P_y^2$ has a wavelength dependency, and its value becomes larger at shorter wavelengths. We get the properties of light at the photocathode of the photo-

(11) O'Handley, R. C. *J. Opt. Soc. Am.* **1973**, *63*, 523–528.

multiplier by matrix multiplication

$$\hat{D} \cdot \frac{1}{2} \begin{pmatrix} 1 \\ 0 \\ \sin(\delta + \alpha) \\ -\cos(\delta + \alpha) \end{pmatrix} =$$

$$\frac{1}{2} \begin{pmatrix} (P_x^2 + P_y^2) + (P_x^2 - P_y^2)\cos 2a \cos(\delta + \alpha) \\ (P_x^2 - P_y^2)\sin 2a + (P_x - P_y)^2 \cos 2a \cos(\delta + \alpha) \\ 2P_xP_y \sin(\delta + \alpha) \\ (P_x^2 - P_y^2)\cos 2a - [(P_x^2 + P_y^2)\cos^2 2a + 2P_xP_y \sin^2 2a] \times \\ \cos(\delta + \alpha) \end{pmatrix}$$

$$(15)$$

What we want is the intensity of light at the detector, $I_d(0)$.

$$I_d(0) =$$
$$(1/2)[(P_x^2 + P_y^2) + (P_x^2 - Py^2)\cos 2a(\cos \delta \cos \alpha -$$
$$\sin \delta \sin \alpha)] = (1/2)[(P_x^2 + P_y^2) + (P_x^2 - P_y^2) \times$$
$$\cos 2a \cos \alpha J_0\delta_m° + (P_x^2 - P_y^2)\cos(2a)2J_2\delta_m° \cos 2W_m t \times$$
$$\cos \alpha - (P_x^2 - P_y^2)\cos(2a)2J_1\delta_m° \sin W_m t \sin \alpha] \quad (16)$$

Thus, the photocurrent consists of dc, W_m, and $2W_m$ components. In the signal processing of the CD spectrophotometer, the dc component of the electric signal is kept at a constant value, $V_{dc}(0)$, independent of the total luminous flux, by a servo control of the photomultiplier power supply. The W_m component processed by a lock-in amplifier in the electronic systems, $V_{ac}(W_m)$, is a signal detected as a CD output. Furthermore, the CD spectrum which appears on a recorder is set as the ratio of the W_m to dc signals, $CD_r = V_{ac}(W_m)/V_{dc}(0)$. Thus,

$$V_{dc}(0) = (P_x^2 + P_y^2) + (P_x^2 - P_y^2)\cos 2a \cos(\alpha)J_0\delta_m° \quad (17)$$

$$V_{ac}(W_m) = (4K/\pi)(P_x^2 - P_y^2)\cos 2a[J_2\delta_m°R(2W_m)\cos \alpha - J_1\delta_m° \text{ sine } \alpha \sin W_m t] \quad (18)$$

$$CD_r = [(4K/\pi)(P_x^2 - P_y^2)\cos 2a[J_2\delta_m°R(2W_m)\cos \alpha - J_1\delta_m° \sin \alpha \sin W_m t]]/[(P_x^2 + P_y^2) + (P_x^2 - P_y^2)\cos \alpha J_0\delta_m°] \quad (19)$$

where K is a response constant related to the gain of the lock-in amplifier. Table III summarizes the values of K for our J-500 CD spectropolarimeter. $R(2W_m)$ is the first harmonic response of the lock-in amplifier. For an ideal lock-in amplifier, $R(2W_m)$ is equal to zero. But, there is, in reality, no ideal lock-in amplifier. This is because a square wave used as the gating signal for the phase sensitive detector (PSD) has not an ideal square-wave form, and consequently PSD responds to the first harmonic up to the order of 10^{-2}. As a result of intensive improvement and careful readjustment of electronic systems, our lock-in amplifier has obtained a first harmonic response of 2×10^{-5}. Ordinary JASCO J-500 CD spectropolarimeters respond to the first harmonic in the order from 10^{-3} to 3×10^{-4}. According to Norden,[2] his JASCO J-40 spectropolarimeter has a first harmonic response of 10^{-2}. Equation 19 is very important because it represents the base-line shift of the CD spectropolarimeter under the conditions of the base-line correction "off" as shown in Figure 2. We also easily understand from this equation that the performance of the CD spectropolarimeter is determined by the following three factors: (1) the polarization characteristics of the photomultiplier ($P_x^2 - P_y^2$), (2) the residual static strain birefringence of the optical modulator, and (3) the first harmonic response of the lock-in amplifier, $R(2W_m)$. This is the reason why the head-on-type photomultiplier should be used instead of the side-on type, and a Kemp type of PEM is preferable.

With the above preparation, let us consider the apparent CD signals observed in the following four cases of cholesteric liquid crystals. In all cases, we regard the cholesteric liquid crystal

(CLC) as build up of a large number of helically arranged thin layers.

Case 1. CLC Build Up of a Large Number of Linearly Birefringent Thin Layers Arranged Helically. For a linearly birefringent layer whose optical axis is aligned parallel to the x axis, the Mueller matrix can be formulized as

$$\hat{S}(0) = e^{-A_e}\begin{pmatrix} 1 & 0 & 0 & 0 \\ 0 & \cos\gamma & -\sin\gamma & 0 \\ 0 & \sin\gamma & \cos\gamma & 0 \\ 0 & 0 & 0 & 1 \end{pmatrix} \quad (20)$$

where A_e is the mean absorbance and γ is the retardation. The intensity of light at the detector can be calculated as the matrix product of $\hat{D}\cdot\hat{S}\cdot\hat{M}_{\delta+\alpha}\cdot\hat{P}\cdot\hat{I}$. Therefore, we obtain

$$I_d = \frac{1}{2}e^{-A_e}((P_x^2 + P_y^2) - (P_x^2 - P_y^2) \times$$
$$[\sin 2a \sin\gamma \sin(\delta + \alpha) + \cos 2a \cos(\delta + \alpha)]) \quad (21)$$

The output to the recorder, CD_r, is given as

$$CD_r = \{-(4/\pi) \times$$
$$(P_x^2 - P_y^2)([J_1\delta_m{}^\circ \sin W_m t \cos\alpha + J_2\delta_m{}^\circ R(2W_m) \sin\alpha] \times$$
$$\sin 2a \sin + [J_2\delta_m{}^\circ R(2R_m) \cos\alpha -$$
$$J_1\delta_m{}^\circ \sin W_m t \sin\alpha] \cos 2a)\}/\{(P_x^2 + P_y^2) - (P_x^2 - P_y^2) \times$$
$$[\sin 2a \sin\gamma J_0\delta_m{}^\circ \sin\alpha + \cos 2a J_0\delta_m{}^\circ \cos 2a]\} \quad (22)$$

As being shown in Figure 3, an apparent CD signal is always observed in the linearly birefringent sample.

Now let us consider a helically arranged pile of linearly birefringent layers in the counterclockwise sense. The pile is composed of n layers. Let the principal axes of the first layer be inclined at an angle θ with respect to $0x$ and $0y$. Then, the Mueller matrix of the first layer is given as

$$\hat{S}_1 = \hat{T}^{-1}(\theta)\cdot\hat{S}(0)\cdot\hat{T}(\theta) \quad (23)$$

where $\hat{T}(\theta)$ is the rotation matrix expressed as

$$\hat{T}(\theta) = \begin{pmatrix} 1 & 0 & 0 & 0 \\ 0 & \cos 2\theta & 0 & -\sin 2\theta \\ 0 & 0 & 1 & 0 \\ 0 & \sin 2\theta & 0 & \cos 2\theta \end{pmatrix} \quad (24)$$

and

$$\hat{T}^{-1}(\theta)\cdot\hat{T}(\theta) = 1 \quad (25)$$

The Mueller matrix for a second layer whose principal axes are inclined at 2θ with respect to $0X$ and $0Y$ is

$$\hat{S}_2 = \hat{T}^{-1}(2\theta)\cdot\hat{S}(0)\cdot\hat{T}(2\theta) \quad (26)$$

Similarly, the Mueller matrix for a nth layer is

$$\hat{S}_n = \hat{T}^{-1}(n\theta)\cdot\hat{S}(0)\cdot\hat{T}(n\theta) \quad (27)$$

We can formulate the Mueller matrix for the pile of n layers as

$$\hat{S} = \hat{S}_n\cdot\hat{S}_{n-1} \dots \hat{S}_2\cdot\hat{S}_1 =$$
$$\hat{T}^{-1}(n\theta)\cdot\hat{S}(0)\cdot\hat{T}(n\theta) \dots \cdot T^{-1}(2\theta)\cdot\hat{S}(0)\cdot\hat{T}(2\theta)T^{-1}\cdot(\theta)\cdot\hat{S}(0)\cdot\hat{T}(\theta) \quad (28)$$

Using $\hat{T}^{-1}(\theta)\cdot\hat{T}(\theta) = 1$, $\hat{T}(2\theta) = \hat{T}(\theta)\cdot\hat{T}(\theta)$, $\hat{T}(3\theta) = \hat{T}(\theta)\cdot\hat{T}(2\theta)$, etc., we get S as

$$\hat{S} = \hat{T}^{-1}(n\theta)\cdot[\hat{S}(0)\cdot\hat{T}(\theta)]^n \quad (29)$$

Here,

$$\hat{T}^{-1}(n\theta) = \begin{pmatrix} 1 & 0 & 0 & 0 \\ 0 & \cos 2n\theta & 0 & -\sin 2n\theta \\ 0 & 0 & 1 & 0 \\ 0 & \sin 2n\theta & 0 & \cos 2n\theta \end{pmatrix} \quad (30)$$

and

$$\hat{S}(0)\cdot T(\theta) = e^{-A_e}\begin{pmatrix} 1 & 0 & 0 & 0 \\ 0 & \cos\gamma \cos 2\theta & -\sin\gamma & -\cos\gamma \sin 2\theta \\ 0 & \sin\gamma \cos 2\theta & \cos\gamma & -\sin\gamma \sin 2\theta \\ 0 & \sin 2\theta & 0 & \cos 2\theta \end{pmatrix} \quad (31)$$

The matrix elements of $[\hat{S}(0)\cdot\hat{T}(\theta)]^n$ become very complicated functions of $\cos\gamma$, $\sin\gamma$, $\sin 2\theta$, and $\cos 2\theta$. However, $\hat{S}$ can be formulized as

$$\hat{S} = e^{-nA_e}\begin{pmatrix} 1 & 0 & 0 & 0 \\ 0 & M_{11} & M_{12} & M_{13} \\ 0 & M_{21} & M_{22} & M_{23} \\ 0 & M_{31} & M_{32} & M_{33} \end{pmatrix} \quad (32)$$

where M_{ij} ($j \neq 0$, $j \neq 0$) are complicated functions expressed as the products of $\cos\gamma$, $\sin\gamma$, $\sin 2\theta$, and $\cos 2\theta$ and have nonzero values. Thus, the light intensity at the detector is obtained from simple matrix calculations as

$$I_d(0) = \frac{1}{2}e^{-nA_e}[(P_x^2 + P_y^2) + (P_x^2 - P_y^2)[(M_{12} \sin 2a +$$
$$M_{32} \cos 2a) \sin(\delta + \alpha) - (M_{13} \sin 2a +$$
$$M_{33} \cos 2a) \cos(\delta + \alpha)]] \quad (33)$$

The W_m and dc components of the electric signals are

$$V_{ac}(W_m) = (4K/\pi)(P_x^2 - P_y^2)[(M_{12} \sin 2a + M_{32} \cos 2a) \times$$
$$[J_1\delta_m{}^\circ \sin W_m t \cos\alpha + J_2\delta_m{}^\circ R(2W_m) \sin\alpha] - (M_{13} \sin 2a$$
$$+ M_{33} \cos 2a) (J_2\delta_m{}^\circ R(2W_m) \cos\alpha - J_1\delta_m{}^\circ \sin W_m t \sin\alpha)] \quad (34)$$

and

$$V_{dc}(0) =$$
$$(P_x^2 + P_y^2) + (P_x^2 - P_y^2)[(M_{12} \sin 2a + M_{32} \cos 2a) \times$$
$$J_0\delta_m{}^\circ \sin\alpha - (M_{13} \sin 2a + M_{33} \cos 2a)J_0\delta_m{}^\circ \cos\alpha] \quad (35)$$

The output to the recorder. $CD_r = V_{ac}(W_m)/V_{dc}(0)$, is not equal to zero. Since $P_x^2 - P_y^2$, a, α, and M_{ij} ($i \neq 0$, $j \neq 0$) all have wavelength dependence, CD_r changes with wavelength.

Case 2. CLC Build Up of Helically Arranged Thin Layers with CB and LB. This case is near to the reality because CLC can be regarded as a helically arranged pile of thin layers of optically active, regularly oriented molecules. Therefore, each layer should have both CB and LB simultaneously. We formulize the Mueller matrix of a circularly and linearly birefringent layer whose optical axis is aligned to the x axis as[7]

$$\hat{S}(0) = e^{-A_e} \times$$
$$\begin{pmatrix} 1 & 0 & 0 & 0 \\ 0 & 1 - \frac{1}{2}(\beta^2 + \gamma^2) & -[\gamma - \frac{1}{6}(\beta^2\gamma + \gamma^3)] & -[(\beta - \frac{1}{6}(\beta\gamma^2 + \beta^3)] \\ 0 & -(\beta^2\gamma + \gamma^3) & 1 - \frac{1}{2}\gamma^2 & -\frac{1}{2}\beta\gamma \\ 0 & -(\beta\gamma^2 + \beta^3) & -\frac{1}{2}\beta\gamma & 1 - \frac{1}{2}\beta^2 \end{pmatrix} \quad (36)$$

where β and γ are circular and linear retardations, respectively.

The Mueller matrix of a right helically arranged pile of n layers is obtained by the same procedure

$$\hat{S}_n = T^{-1}(n\theta)\cdot[\hat{S}(0)\cdot\hat{T}(\theta)]^n$$

$\hat{S}$ can be formulized as

$$\hat{S} = e^{-nA_e}\begin{pmatrix} 1 & 0 & 0 & 0 \\ 0 & M_{11} & M_{12} & M_{13} \\ 0 & M_{21} & M_{22} & M_{23} \\ 0 & M_{31} & M_{32} & M_{33} \end{pmatrix} \quad (37)$$

where the matrix elements M_{ij} ($i \neq 0$, $j \neq 0$) are very complicated functions of β, γ, $\sin 2\theta$, and $\cos 2\theta$. Thus, the light intensity at the detector is

$$I_d(0) =$$
$$\frac{1}{2}e^{-nA_e}[(P_x^2 + P_y^2) - (P_x^2 - P_y^2)((M_{12} \sin 2a + M_{32} \times$$
$$\cos 2a) \sin(\delta + \alpha) - (M_{13} \sin 2a + M_{33} \cos 2a)\cos(\delta + \alpha))] \quad (38)$$

The W_m and dc components of the electric signal are

$$V_{ac}(W_m) = (4K/\pi)(P_x^2 - P_y^2)[(M_{12} \sin 2a + M_{32} \cos 2a) \times$$
$$[J_1\delta_m{}^\circ \sin W_m t \cos\alpha + J_2\delta_m{}^\circ R(2W_m) \sin\alpha] - (M_{13} \sin 2a$$
$$+ M_{33} \cos 2a) (J_2\delta_m{}^\circ R(2W_m) \cos\alpha - J_1\delta_m{}^\circ \sin W_m t \sin\alpha)] \quad (39)$$

$$V_{dc}(0) =$$
$$(P_x^2 + P_y^2) + (P_x^2 - P_y^2)[(M_{12} \sin 2a + M_{32} \cos 2a) \times$$
$$J_0\delta_m \sin\alpha - (M_{13} \sin 2a + M_{33} \cos 2a)J_0\delta_m{}^\circ \cos\alpha] \quad (40)$$

Also here the output to the recorder, $CD_r = V_{ac}(W_m)/V_{dc}(0)$, has

nonzero values which are dependent upon the wavelength, because $P_x^2 - P_y^2$, a, α, and M_{ij} change with wavelength.

We consider that typical examples of this case are the CD spectra observed in a jelly of chiral 12-hydroxyoctadecanoic acid[12] and in a liquid crystal of N-acylamino acids and organic solvents.[13]

The above two cases, the apparent CD appears because of the polarization characteristics of the detector, i.e., nonzero $P_x^2 - P_y^2$. With an ideal detector, there will be no apparent CD. But as there is no ideal detector, an apparent CD is inevitable in the above cases. We should emphasize that these apparent CD spectra are completely different from those originating from a selective reflection of circularly polarized light.[14-16] These are due to the coupling of anisotropic media and nonideal optics and electronics of the CD spectropolarimeters.

Case 3. CLC Build Up of Helically Arranged Thin Layers with LB and LD. We can formulize the Mueller matrix for a linearly birefringent and dichroic thin layer whose optical axis is at the x axis[4]

$$\hat{S} = e^{-A}e\begin{pmatrix} \cosh LD & 0 & 0 & -\sinh LD \\ 0 & \cos\gamma & -\sin\gamma & 0 \\ 0 & \sin\gamma & \cos\gamma & 0 \\ -\sinh LD & 0 & 0 & \cosh LD \end{pmatrix} \quad (41)$$

where LD is the $x - y$ linear dichroism. By the same procedure, we can get the Mueller matrix of a right helically arranged pile of n layers as

$$\hat{S}_n = \hat{T}^{-1}(n\theta)\cdot[\hat{S}(0)\cdot\hat{T}(\theta)]^n$$

$\hat{S}$ can be formulized as

$$\hat{S} = e^{-nA}e\begin{pmatrix} M_{00} & M_{01} & M_{02} & M_{03} \\ M_{10} & M_{11} & M_{12} & M_{13} \\ M_{20} & M_{21} & M_{22} & M_{23} \\ M_{30} & M_{31} & M_{32} & M_{33} \end{pmatrix} \quad (42)$$

where the matrix elements, M_{ij}, are very complicated functions of LD, γ, $\sin 2\theta$, and $\cos 2\theta$.

The intensity at the detector is

$I_d(0) =$

$(\frac{1}{2})e^{-nA}e[(P_x^2 + P_y^2)[M_{00} + M_{02}\sin(\delta + \alpha) - M_{03}\cos(\delta + \alpha)] + (P_x^2 - P_y^2)[\sin 2a[M_{10} + M_{12}\sin(\delta + \alpha) - M_{13}\cos(\delta + \alpha)] + \cos 2a(M_{30} + M_{32}\sin(\delta + \alpha) - M_{33}\cos(\delta + \alpha))]]$

$$(43)$$

The W_m and dc components of the electric signal are

$V_{ac}(0^\circ, W_m) = (4K/\pi)[[(P_x^2 + P_y^2)M_{02} + (P_x^2 - P_y^2)[M_{12} \times \sin 2a + M_{32}\cos 2a][J_1\delta_m^\circ \sin W_m t \cos\alpha + J_2\delta_m^\circ R(2W_m) \times \sin\alpha] - [(P_x^2 + P_y^2)M_{03} + (P_x^2 - P_y^2)(M_{13}\sin 2a + M_{33}\cos 2a)][J_2\delta_m^\circ R(2W_m)\cos\alpha - J_1\delta_m^\circ \sin W_m t \sin\alpha)]]$

$$(44)$$

$V_{dc}(0) =$

$(P_x^2 + P_y^2)[M_{00} + M_{02}\delta_m^\circ \sin\alpha - M_{02}J_0\delta_m^\circ \cos\alpha] + (P_x^2 - P_y^2)[[M_{10} + M_{12}J_0\delta^\circ \sin\alpha - M_{13}J_0\delta_m^\circ \cos\alpha]\sin 2a + [M_{30} + M_{32}J_0\delta_m^\circ \sin\alpha - M_{33}J_0\delta_m^\circ \cos\alpha]\cos 2a] \quad (45)$

The output to the recorder, $CD_r = V_{ac}(W_m)/V_{dc}$, has nonzero value which depends upon the wavelength. This value is obviously much larger than that in the cases 1 and 2.

Let us investigate the following example in detail to understand the situation of how the apparent CD signals appear in this case. Consider a helically arranged pile composed of eight thin layers which are linearly birefringent and dichroic. The principal axes of the successive layers are turned through 45° degree to make

(12) Tachibana, T.; Mori, T.; Hori, K. *Nature (London)* **1979**, *278*, 578–579.

(13) Sakamoto, K.; Yoshida, R.; Hatano, M.; Tachibana, T. *J. Am. Chem. Soc.* **1978**, *100*, 6898–6902.

(14) Fergason, J. L. *Mol. Cryst.* **1966**, *1*, 293–307.

(15) Conners, G. H. *J. Opt. Soc. Am.* **1968**, *58*, 875–879.

(16) Chandrasekhar, S.; Srivivasa Rao, K. N. *Acta Crystallogr., Sect. A* 1968, *A24*, 445–451.

one turn of the left-handed helix of pitch. The linear retardation γ and linear dichroism η are assumed to be small. We can formulize the Mueller matrix for a linearly birefringent and dichroic layer whose principal axis is at the x axis as follows

$$\hat{S}(0) = e^{-A}e\begin{pmatrix} \cosh\eta & 0 & 0 & -\sinh\eta \\ 0 & \cos\gamma & -\sin\gamma & 0 \\ 0 & \sin\gamma & \cos\gamma & 0 \\ -\sinh\eta & 0 & 0 & \cosh\eta \end{pmatrix} \quad (46)$$

Since γ and η are small, we can take $\cos\gamma = 1$ and $\cosh\eta = 1$. Therefore, the Mueller matrices of these eight layers are given as

$$\hat{S}(0^\circ) = e^{-A}e\begin{pmatrix} 1 & 0 & 0 & -a \\ 0 & 1 & -b & 0 \\ 0 & b & 1 & 0 \\ -a & 0 & 0 & 1 \end{pmatrix} \quad (47)$$

$$\hat{S}(45^\circ) = e^{-A}e\begin{pmatrix} 1 & -a & 0 & 0 \\ -a & 1 & 0 & 0 \\ 0 & 0 & 1 & -b \\ 0 & 0 & b & 1 \end{pmatrix} \quad (48)$$

$$\hat{S}(90^\circ) = e^{-A}e\begin{pmatrix} 1 & 0 & 0 & a \\ 0 & 1 & b & 0 \\ 0 & -b & 1 & 0 \\ a & 0 & 0 & 1 \end{pmatrix} \quad (49)$$

$$\hat{S}(135^\circ) = e^{-A}e\begin{pmatrix} 1 & a & 0 & 0 \\ a & 1 & 0 & 0 \\ 0 & 0 & 1 & b \\ 0 & 0 & -b & 1 \end{pmatrix} \quad (50)$$

$$\hat{S}(180^\circ) = e^{-A}e\begin{pmatrix} 1 & 0 & 0 & -a \\ 0 & 1 & -b & 0 \\ 0 & b & 1 & 0 \\ -a & 0 & 0 & 1 \end{pmatrix} \quad (51)$$

$$\hat{S}(225^\circ) = e^{-A}e\begin{pmatrix} 1 & -a & 0 & 0 \\ -a & 1 & 0 & 0 \\ 0 & 0 & 1 & -b \\ 0 & 0 & b & 1 \end{pmatrix} \quad (52)$$

$$\hat{S}(270^\circ) = e^{-A}e\begin{pmatrix} 1 & 0 & 0 & a \\ 0 & 1 & b & 0 \\ 0 & -b & 1 & 0 \\ a & 0 & 0 & 1 \end{pmatrix} \quad (53)$$

$$\hat{S}(315^\circ) = e^{-A}e\begin{pmatrix} 1 & a & 0 & 0 \\ a & 1 & 0 & 0 \\ 0 & 0 & 1 & b \\ 0 & 0 & -b & 1 \end{pmatrix} \quad (54)$$

where A_e is the mean absorbance of a layer, $a = \sinh\eta$, and $b = \sin\gamma$. Consequently, the Mueller matrix of a left-handed helical pile is

$\hat{S} = \hat{S}(315^\circ)\cdot\hat{S}(270^\circ)\cdot\hat{S}(225^\circ)\cdot\hat{S}(180^\circ)\cdot\hat{S}(135^\circ)\cdot\hat{S}(90^\circ)\cdot\hat{S}(45^\circ)\cdot\hat{S}(0^\circ) =$

$$e^{-A}e\begin{pmatrix} 1 - 4a^2 & 2ab^2 & 4ab & 2a^3 - 2ab^2 \\ 2ab^2 & 1 - 2a^2 + 2b^2 & 4a^2b & 2a^2 - 2b^2 \\ 4ab & -2a^2b + 3b^3 & 1 + 4b^2 & -4a^2b \\ -4ab^2 & -2a^2 + 2b^2 & -2b^3 + 2a^2b & 1 - 2a^2 + 2b^2 \end{pmatrix}$$

$$(55)$$

The intensity at the detector is given as

$I_d(0) = (\frac{1}{2})e^{-A}e[(P_x^2 + P_y^2)[1 - 4\sinh^2\eta - 4\sinh\eta\sin\gamma\sin(\delta + \alpha) - 2(\sinh^3\eta - \sinh\eta\sin^2\gamma)\cos(\delta + \alpha)] + (P_x^2 - P_y^2)[[2\sinh\eta\sin^2\delta + 4\sinh^2\eta\sin\delta\sin(\delta + \alpha) - 2(\sinh^2\eta - \sin^2\gamma)\cos(\delta + \alpha)]\sin 2a + [-4\sinh\eta\sin^2\delta - 2(\sinh^2\eta\sin\gamma - \sin^3\gamma)\sin(\delta + \alpha) - (1 - 2\sinh^2\eta + 2\sin^2\gamma)\cos(\delta + \alpha)]\cos 2a]] \quad (56)$

$$\hat{S} = e^{-A}e \begin{pmatrix} 1 + \frac{1}{2}\eta^2 & -\frac{1}{2}\beta\eta & -\frac{1}{6}\beta\gamma\eta & -\eta + \frac{1}{6}(\beta^2\eta - \eta^3) \\ \frac{1}{2}\beta\eta & 1 - \frac{1}{2}(\beta^2 + \eta^2) & -\gamma + \frac{1}{6}(\gamma^3 + \beta\gamma^2) & -\beta + \frac{1}{6}(\beta\gamma^2 + \beta^3 - \beta\eta^2) \\ \frac{1}{6}\beta\gamma\eta & \gamma - \frac{1}{6}(\beta^2\gamma + \gamma^3) & 1 - \frac{1}{2}\gamma^2 & -\frac{1}{2}\beta\gamma \\ -\eta + \frac{1}{6}(\beta^2\eta - \eta^3) & \beta - \frac{1}{6}(\beta^3 + \beta\gamma^2 - \beta\eta^2) & -\frac{1}{2}\beta\gamma & 1 + \frac{1}{2}(\eta^2 - \beta^2) \end{pmatrix} \quad (63)$$

The W_m and dc components of the electric signal are

$V_{ac}(W_m) = (4K/\pi)[[-4(P_x^2 + P_y^2) \sinh \eta \sin \gamma + (P_x^2 - P_y^2)[4 \sinh^2 \eta \sin \gamma \sin 2a + 2(\sinh^2 \eta \sin^3 \delta - \sin \delta) \cos 2a][J_1\delta_m^{\circ} \sin W_m t \cos \alpha + J_2\delta_m^{\circ}R(2W_m) \sin \alpha] - [2(P_x^2 + P_y^2)(\sinh^3 \eta - \sinh \eta \sin^2 \gamma) - (P_x^2 - P_y^2) \times [2(\sinh^2 \eta - \sin^2 \gamma) \sin 2a + (1 - 2 \sinh^2 \eta + 2 \sin^2 \gamma) \cos 2a)][J_2 \delta_m^{\circ}R(2W_m) \cos \alpha - J_1\delta_m^{\circ} \sin W_m t \sin \alpha]$ (57)

$V_{dc} = (P_x^2 + P_y^2)[1 - 4 \sinh^3 \eta + 4 \sinh \eta \sin \gamma J_0\delta_m^{\circ} \sin \alpha - 2(\sinh^3 \eta - \sinh \eta \sin^2 \gamma)J_0\delta_m^{\circ} \cos \alpha] + (P_x^2 - P_y^2)[[2 \sinh \eta \sin^2 \delta + 4 \sinh^2 \eta \cos \gamma J_0\delta_m^{\circ} \sin \alpha + 2(\sinh^2 \eta - \sin^2 \gamma)J_0\delta_m^{\circ} \cos \alpha] \sin 2a + [4 \sinh \eta \sin^2 \gamma + 2(\sinh^2 \eta \sin \gamma - \sin^3 \delta)J_0\delta_m^{\circ} \sin \alpha + (1 - 2 \sinh^2 \eta + 2 \sin^2 \gamma)J_0 \delta_m^{\circ} \cos \alpha] \cos 2a]$ (58)

The apparent CD spectra, $CD_r = V_{ac}(W_m)/V_{dc}$, which have fairly large amplitudes are not related at all to the CD but are due to the LB and LD. Furthermore, since the Mueller matrix of the helical pile is independent of rotation around the x axis, no change in the apparent CD spectrum can be detected when the helical pile is rotated around the light beam. Thus, we cannot conclude in this case that no LD contribution to the CD band can be observed.

Now, let us consider a right-handed helical pile. By the same matrix multiplication, we can obtain

$$\hat{S} = e^{-A}e \begin{pmatrix} 1 - 4a^2 & -4ab^2 & -4ab & 2a^3 - 2ab^2 \\ 2a^3 - 2ab^2 & 1 - 2a^2 + 2b^2 & 4a^2b & -2a^2 + 2b^2 \\ -4ab & -2a^2b + 2b^3 & 1 + 4b^2 & -b^3 - a^2b \\ -4ab^2 & 2a^2 - 2b^2 & 2b^3 - 2a^2b & 1 - 2a^2 + 2b^2 \end{pmatrix}$$
(59)

Consequently, the light intensity at the detector is

$I_d(0) = (\frac{1}{2})e^{-A}e((P_x^2 + P_y^2)[1 - 4 \sinh^2 \eta - 4 \sinh \eta \sin \gamma \sin (\delta + \alpha) - 2(\sinh^3 \eta - \sinh \eta \sin^2 \gamma) \cos (\delta + \alpha)] + (P_x^2 - P_y^2)[[2(\sinh^3 \eta - \sinh \eta \sin^2 \gamma) + 4 \sinh^2 \eta \times \sin^2 \gamma \sin (\delta + \alpha) + 2(\sinh^2 \eta - \sin^2 \gamma) \cos (\delta + \alpha)] \sin 2a + [-4 \sinh \eta \sin^2 \gamma + 2(\sin^3 \gamma - \sinh^2 \eta \sin \gamma) \sin (\delta + \alpha) - (1 - 2 \sinh^2 \eta + 2 \sin^2 \gamma) \cos (\delta + \alpha)] \cos 2a]]$ (60)

The W_m and dc components of the electric signal are

$V_{ac}(W_m) = (4K/\pi)[[-4(P_x^2 + P_y^2) \sinh \eta \sin \gamma + (P_x^2 - P_y^2)[4 \sinh^2 \eta \sin \gamma \sin 2a + 2(\sin^3 \gamma - \sinh^2 \eta \sin \gamma) \cos 2a][J_1\delta_m^{\circ} \sin W_m t \cos \alpha + J_2\delta_m^{\circ}R(2W_m) \times \sin \alpha] - [2(P_x^2 + P_y^2)(\sinh^3 \eta - \sin^2 \gamma \sinh \eta) - (P_x^2 - P_y^2) \times [2(\sinh^2 \eta - \sin^2 \gamma) \sin 2a - (1 - 2 \sinh^2 \eta + 2 \sin^2 \gamma) \cos 2a)] \times [J_2\delta_m^{\circ}R(2W_m) \cos \alpha - J_1\delta_m^{\circ} \sin W_m t \sin \alpha]$ (61)

$V_{dc} = (P_x^2 + P_y^2)[1 - 4 \sinh^2 \eta - 4 \sinh \eta \sin \gamma J_0\delta_m^{\circ} \sin \alpha - 2(\sinh^3 \eta - \sinh \eta \sin^2 \gamma)J_0\delta_m^{\circ} \times \cos \alpha] + (P_x^2 - P_y^2)[[2(\sinh^3 \eta - \sinh \eta \sin^2 \gamma) + 4 \sinh^2 \eta \times \sin \gamma J_0\delta_m^{\circ} \sin \alpha + 2(\sinh^2 \eta - \sin^2 \gamma)J_0\delta_m^{\circ} \cos \alpha] \sin 2a + [-4 \sinh \eta \sin^2 \gamma + 2(-\sinh^2 \eta \sin \gamma + \sin^3 \gamma)J_0\delta_m^{\circ} \sin \alpha - (1 - 2 \sinh^2 \eta + 2 \sin^2 \gamma)J_0\delta_m^{\circ} \cos \alpha]] \cos 2a]]$ (62)
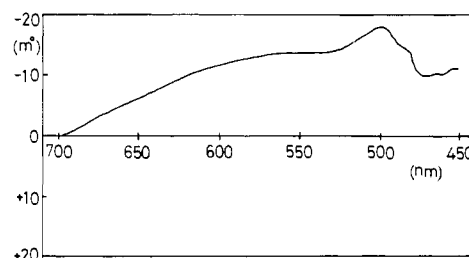

Figure 3. Apparent CD spectrum observed for a Polaroid plastic film $\lambda/4$-in. plate.

The output to the recorder, $CD_r = V_{ac}(W_m)/V_{dc}$, is opposite in sign but about equal in magnitude to that of the left-handed helical pile. These situations correspond to the cholesteric liquid crystals of L- and R-enantiomers.

Case 4. CLC Build Up of a Large Number of Helically Arranged Thin Layers with CB, LB, and LD. This is the same as the case that achiral dye molecules are dissolved in cholesteric liquid crystals composed of optically active molecules which are oriented regularly. In other words, this is the situation in which the LCICD is observed. We can express a circularly and linearly birefringent and linearly dichroic thin layer with its optical axis at the x axis as shown in eq 63. The intensity of light at the detector is given as

$I_d(0) = \frac{1}{2}e^{-A}e[(P_x^2 + P_y^2)[(1 + \frac{1}{2}\eta^2) + \frac{1}{6}\beta\gamma\eta \times \sin (\delta + \alpha) + (\eta - \frac{1}{6}(\beta^2\eta - \eta^3)) \cos (\delta + \alpha)] + (P_x^2 - P_y^2)[\frac{1}{2}\beta\eta - (\delta - \frac{1}{6}(\gamma^3 + \beta^2\gamma)) \sin (\delta + \alpha) + (\beta - \frac{1}{6}(\beta\gamma^2 + \beta^3 - \beta\eta^2))\cos(\delta + \alpha) \sin 2a + (P_x^2 - P_y^2)[-\eta + \frac{1}{6}(\beta^2\eta - \eta^3) - \frac{1}{2}\beta\gamma \sin (\delta + \alpha) - (1 + \frac{1}{2}(\eta^2 - \beta^2)) \cos (\delta + \alpha)] \cos 2a]$ (64)

The W_m and dc components of the electric signal are

$V_{ac}(W_m) = (4K/\pi)[[\frac{1}{6}(P_x^2 + P_y^2)\beta\gamma\eta - (P_x^2 - P_y^2)[(\gamma - \frac{1}{6}(\gamma^3 + \beta^2\gamma)) \sin 2a + \frac{1}{2} \cos 2a\cdot\beta\gamma][J_1\delta_m^{\circ} \sin W_m t \cos \alpha + J_2\delta_m^{\circ}R(2W_m) \sin \alpha] +[(P_x^2 + P_y^2) \times (\eta - \frac{1}{6}(\beta^2\eta - \eta^3)) + (P_x^2 - P_y^2) \sin 2a (\beta - \frac{1}{6}(\beta\gamma^2 + \beta^3 - \beta\eta^2)) - (P_x^2 - P_y^2) \cos 2a(1 + \frac{1}{2}(\eta^2 - \beta^2)][J_2\delta_m^{\circ}R(2W_m) \times \cos \alpha - J_1\delta_m^{\circ} \sin W_m t \sin \alpha]$ (65)

$V_{dc} = (P_x^2 + P_y^2)[(1 + \frac{1}{2}\eta^2) + \frac{1}{6}\beta\gamma\eta J_0\delta_m^{\circ} \sin \alpha + (\eta - \frac{1}{6}(\beta^2\eta - \eta^3))J_0\delta_m^{\circ} \cos \alpha] + (P_x^2 - P_y^2)[[\frac{1}{2}\beta\eta - (\gamma - \frac{1}{6}(\gamma^3 + \beta^2\gamma))]J_0\delta_m^{\circ} \sin \alpha + [\beta - \frac{1}{6}(\beta\gamma^2 + \beta^3 - \beta\eta^2)]J_0\delta_m^{\circ} \cos \alpha] \sin 2a + (P_x^2 - P_y^2)[(-\eta + \frac{1}{6}(\beta^2\eta - \eta^3) - \frac{1}{2}\beta\gamma)J_0\delta_m^{\circ} \sin \alpha - (1 + \frac{1}{2}(\eta^2 - \beta^2))J_0\delta_m^{\circ} \cos \alpha] \cos 2a$ (66)

The output to the recorder, $CD_r = V_{ac} (W_m)/V_{dc}$, has fairly large nonzero values which change with wavelength. Furthermore, this does not have any relation to CD. Thus, in this case, the CD signal being observed even in a single layer is not due to the optical activity induced in achiral molecules.

We can obtain the Mueller matrix of helically arranged pile of n layers as

$$\hat{S}_n = \hat{T}^{-1}(n\theta)\cdot[\hat{S}(0)\cdot\hat{T}(\theta)]^n$$

$\hat{S}$ can be formulized as

$$\hat{S} = e^{-nA}e \begin{pmatrix} M_{00} & M_{01} & M_{02} & M_{03} \\ M_{10} & M_{11} & M_{12} & M_{13} \\ M_{20} & M_{21} & M_{22} & M_{23} \\ M_{30} & M_{31} & M_{32} & M_{33} \end{pmatrix} \quad (67)$$

where the matrix elements M_{ij} are very complicated functions of β, γ, η, sin 2θ, and cos 2θ. The light intensity at the detector is

$$I_d(0) =$$

$$\tfrac{1}{2}e^{-nA_c}[[(P_x{}^2 + P_y{}^2)[M_{00} + M_{02}\sin(\delta + \alpha) - M_{03}\cos(\delta + \alpha)] + (P_x{}^2 - P_y{}^2)[\sin 2a[M_{10} + M_{12}\sin(\delta + \alpha) - M_{13}\cos(\delta + \alpha)] + \cos 2a[M_{30} + M_{32}\sin(\delta + \alpha) - M_{33}\cos(\delta + \alpha)]]]$$

(68)

The W_m and dc components of the electric signal are

$$V_{ac}\,(0°,\,W_m) = (4K/\pi)[[(P_x{}^2 + P_y{}^2)M_{02} + (P_x{}^2 - P_y{}^2)[M_{12}\sin 2a + M_{32}\cos 2a]\cdot$$
$$[J_1\delta_m° \sin W_m t \cos \alpha + J_2\delta_m° R(2W_m)\sin \alpha] - [(P_x{}^2 + P_y{}^2)M_{03} + (P_x{}^2 - P_y{}^2)(M_{13}\sin 2a + M_{33}\cos 2a)][J_2\delta_m° R(2W_m)\cos \alpha - J_1\delta_m° \sin W_m t \sin \alpha]]$$

(69)

$$V_{dc}(0) =$$
$$(P_x{}^2 + P_y{}^2)[M_{00} + M_{02}J_0\delta_m° \sin \alpha - M_{02}J_0\delta_m° \cos \alpha] + (P_x{}^2 - P_y{}^2)[[M_{10} + M_{12}J_0\delta_m° \sin \alpha - M_{13}J_0\delta_m° \cos \alpha] \times \sin 2a + [M_{30} + M_{32}J_0\delta_m° \sin \alpha - M_{33}J_0\delta_m° \cos \alpha]\cos 2a]$$

(70)

The output to the recorder, $CD_r = V_{ac}\,(W_m)/V_{dc}$, is not equal to zero. Thus, there is the apparent CD spectra having no relation to the CD in any aspects. The rotation of the helical pile around the light beam induces no "CD" sign change in the apparent CD spectra because of its helical structure. Thus, we can never conclude from the apparent CD spectra that the optically inactive molecules become chiral when dissolved in cholesteric liquid crystals.

Conclusion

The above considered cases show clearly that there may be several obscure points in LCICD data reported so far in the literature. We cannot deny completely the possibility that achiral molecules becomes optically active in cholesteric liquid crystals. But the apparent CD spectra observed in cholesteric liquid crystals with commercially available CD spectrophotometers can generally not provide us with the proof that the optical activity is induced in achiral molecules. Other methods besides CD spectroscopy are therefore necessary to confirm experimentally the presence of the induced optical activity in optically inactive molecules.

Finally, let us give a bit of advice to persons who intend to study induced CD in possibly anisotropic systems. Read the book on polarized light,[8] a paper on the Mueller matrix approach to the polarization–modulation spectroscopy,[4,17] and a number of papers on problems of CD spectropolarimeters[2,3,6,7,9,10] before starting work. We believe it is essential to fully understand the real meanings of the signal which will be observed.

We are going to comment on fluorescence detected circular dichroism in the next paper.

(17) Schonhofer, A.; Kuball, H. G.; Puebla, C. *Chem. Phys.* **1983**, *76*, 453–467.

Adsorption and Decomposition of Dimethyl Methylphosphonate on an Aluminum Oxide Surface

**M. K. Templeton and W. H. Weinberg***

Contribution from the Division of Chemistry and Chemical Engineering, California Institute of Technology, Pasadena, California 91125. Received July 6, 1984

Abstract: The adsorption of gaseous dimethyl methylphosphonate (DMMP) on aluminum oxide film surfaces has been investigated with inelastic electron tunneling spectroscopy. Surface temperatures ranged between 200 and 673 K, and exposures ranged between 3×10^{-4} and 10 torr·s. Tunneling spectra of deuterium-labeled DMMP, methyl alcohol-d_4, methyl methylphosphonate, methylphosphonic acid, and trimethylphosphine oxide, all adsorbed on aluminum oxide surfaces, were used to clarify the structures of the species resulting from the adsorption and decomposition of DMMP. At 200 K, DMMP is adsorbed molecularly with high surface coverages. At surface temperatures above 295 K, DMMP is adsorbed dissociatively in low coverages. Surface temperatures above 473 K lead to the dealkylation of the adspecies, resulting in the formation of adsorbed methylphosphonate.

I. Introduction

The interaction between phosphonate esters and aluminum oxide surfaces is important in two contexts. Not only does it elucidate the surface chemistry of phosphorus/metal oxide systems but it also serves to clarify the chemical nature of the aluminum oxide surface. Perhaps the foremost method for probing surface properties of oxides is through the use of adsorbates. The adsorptions of Lewis and Brønsted bases, such as pyridine and ammonia, were among the first methods used to probe the acid/base properties of aluminum oxide.[1] However, adsorption studies are by no means limited to examining acid/base properties. For example, the adsorption of alcohols, aldehydes, and ketones has been used to demonstrate the nucleophilic character of oxygen atoms on aluminum oxide.[2–4] The adsorption of phosphonate

Scheme I
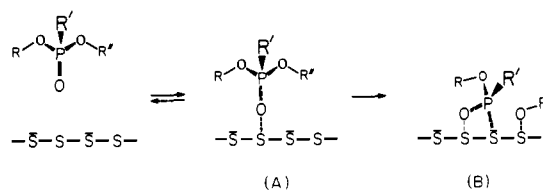
esters can potentially add to the overall understanding of surface chemical properties and their interrelation, since these esters can serve as Lewis bases, modifiers of surface acidity, and/or centers for nucleophilic substitution. For example, the phosphonate ester

(1) L. H. Little, "Infrared Spectra of Adsorbed Species", Chapter 7, Academic Press, New York, 1966, p 180, and references therein.
(2) R. G. Greenler, *J. Chem. Phys.*, 37, 2094 (1962).
(3) H. E. Evans and W. H. Weinberg, *J. Chem. Phys.*, 71, 1537 (1979).
(4) A. V. Deo, T. T. Chuang, and I. G. Dalla Lana, *J. Phys. Chem.* 75, 234 (1971).